Research Paper
J. Astron. Space Sci. 34(1), 37-44 (2017)
https://doi.org/10.5140/JASS.2017.34.1.37

JASS Journal of Astronomy and Space Sciences

Quasi-Periodic Oscillation of a Magnetic Cataclysmic Variable, DO Draconis

Kiyoung Han[1], Yonggi Kim[1,2†], Ivan L. Andronov[3], Joh-Na Yoon[1,2], Lidia L. Chinarova[4]

[1]Chungbuk National University Observatory, Jinchoen 27867, Korea
[2]Department of Astronomy and Space Science, Chungbuk National University, Cheongju 28644, Korea
[3]Department of High and Applied Mathematics, Odessa National Maritime University, Odessa 65029, Ukraine
[4]Astronomical Observatory, Odessa National University, Odessa 65014, Ukraine

In this paper, analysis results of the photometric data of DO Dra will be presented. DO Dra had been observed with 1 m LOAO telescope and 0.6 m CBNUO telescope from 2005 through 2014. The data shows kind of periodic oscillation behavior in the orbital period and also in the spin period. It has been found that these QPOs are not observed always and that the periods vary from 30 min to 80 min. We also found that the period variation seems to repeat itself with the period of 13.5 days. It is essential to monitor this object in the future as well as to carry out model calculation in order to have better understanding of these QPO phenomena.

Keywords: quasi-periodic oscillation, period variation, magnetic cataclysmic variables, DO Dra

1. INTRODUCTION

Cataclysmic variables (CVs) are close binary system in which matters are transferred from the Roche lobe-filling secondary star of late-type to the white dwarf primary. When the secondary evolves to fill up the Roche lobe, matter moves to the primary through Lagrangian point (L1) located inside the system and matter-accretion occurs. In case the white dwarf shows significant strength of magnetic fields, it is called magnetic cataclysmic variable stars (MCVs) and MCVs are classified into intermediate polars (IPs or DQ Her) or polars (or AM Her) depending on the magnetic field strength

In the polars, the magnetic strength of white dwarf is so strong that it hiders the formation of accretion-disk and matter passing Lagrangian point accumulates directly on the surface of the white dwarf along the magnetic field lines. However, in the IPs, the magnetic field is not strong enough, thus, the matter through the Lagrangian point forms the accretion disk; from the inner periphery of the accretion disk, the matter falls onto the surface of the white dwarf along the magnetic field lines.

DO Dra was first categorized as a CV by Patterson et al. (1982) and observed as such at Palomar-Green Survey. At first, it was registered as PG 1140+ 719. Wenzel (1983) observed a phenomenon of explosion in PG 1140+ 719 region which enhanced the brightness by 5 times and recovered the original brightness in 4 days and classified it as a dwarf nova with long periods. Since then, the formal name assigned to PG 1140+ 719 became DO Dra (Samus et al. 2017). While Norton et al. (1999) classified DO Dra as an IP-type, DO Dra is believed to be a complex star which has magnetic fields and generates ejections.

Patterson et al. (1992) discovered the period of 550±3 sec with double peak structure, and Haswell et al. (1997) determined $P_{\rm spin} = 529.^{s}31(2)$, $P_{orb} = 0.^{d}16537398(17)$, the secondary mass, $M_2 = 0.375(14)M_{\odot}$, the primary star mass, $M_{wd} = 0.83(10)M_{\odot}$, and the inclination, $i = 45(4)°$. Šimon (2000) discovered the ejection period of 870 day, and the magnitude decrease rate faster than that of non-magnetic structure. Andronov et al. (2008) identified the ejection periods of 311 day ~ 422 day using the observation data obtained in 2006 ejection and confirmed that the quasi-periodic oscillations (QPOs) also exist in DO Dra.

Received 21 JAN 2017 **Revised** 9 MAR 2017 **Accepted** 9 MAR 2017
†**Corresponding Author**
Tel: +82-43-261-3202, E-mail: ykkim153@chungbuk.ac.kr
ORCID: https://orcid.org/0000-0002-9532-1653

QPOs are phenomena of magnitude variation typically encountered in the X-ray binary star system. *Rossi X-Ray Timing Explorer* (*RXTE*) discovered QPOs with the frequency from 0.001 Hz to 450 Hz (Remillard et al. 2002). QPOs of a white dwarf accompany the non-periodical oscillation of magnitude with the interval of a few min to dozens of min. Recently, on the characteristics of QPOs in the X-Ray region and the optical region for polar-type magnetic white dwarfs, Bonnet-Bidaud et al. (2015) have suggested that QPOs with short periods of 1 sec ~ 3 sec are formed by shock waves. Also, Busschaert et al. (2015) have provided an explanation that QPOs show different behavior in the region of bremsstrahlung only compared to the region where both the cyclotron radiation and the bremsstrahlung radiation occur at the same time through numerical modeling to explain the observation data. QPOs were also observed at TT Ari (Tremko et al. 1996; Andronov et al. 1999; Smak 2014), and while QPOs in IP-type stars are believed to be generated by the bright bulb around the white dwarf with magnetic fields, detailed numerical calculation results have not been reported yet. These QPOs were discovered at DO Dra and Andronov et al. (2008) also discovered disappearance of the QPOs at DO Dra and proposed to name this phenomenon as transient-periodic oscillations (TPOs).

The optical monitoring of MCVs has been performed in Korea since 1995 using domestic telescopes and as a part of "Inter-Longitude Astronomy" campaign (Andronov et al. 2010), international observation monitoring was conducted and the analysis results have been reported (Andronov et al. 2008, 2011, 2015; Kim et al. 2004, 2005a, 2005b, 2009; Yun et al. 2011)

While DO Dra, one of the target stars of ILA campaign, shows variable amplitude and ejection behavior with indeterminable periods, various periods and QPO phenomena obtained from photometric observation data of DO Dra have been analyzed and the results are presented in this study.

2. OBSERVATION AND DATA ANALYSIS

Photometric observation data of DO Dra had been obtained from Mt. Lemmon optical astronomy observatory (LOAO) and Chungbuk national university observatory (CBNUO) for about 10 years from 2005 till 2014. The LOAO telescope located at Mt. Lemmon in Arizona is 1.0 m in diameter and the effective focal ratio is f/7.5. It is mounted on a fork equatorial mount and adopts CCD with 0.64 arcsec/pixel, 2k × 2k resolution, and its field of view (FOV) is 22'.2 × 22'.2. The telescope at CBUNO is 0.6 m in diameter and its optical system is an R-C type with effective focal ratio of f/2.92. in 2012, a CCD with wide FOV of 72' × 72' and 4k × 4k (4096×4096) pixel resolution was been installed. In Fig. 1, a finding map from LOAO including 9 comparison stars is shown and in Table 1, all the relevant data for comparison stars considered in this study are listed. The journal of observations are listed in Appendix I and II.

The IRAF/DAOPHOT package (Massey & Davis 1992) is used to determine instrumental magnitudes of the variable star as well as comparison stars. Using MCV computer program by Andronov & Baklanov (2004) which uses the method of multiple comparison stars (Kim et al. 2004), the final magnitudes are determined. The method of multiple comparison stars allows to estimate an independent brightness of comparison stars in the vicinity of the variable star. The primary comparison star is selected as C1 and its magnitude is $15.^{m}082$ for B filter, $14.^{m}28$ for V filter (Henden & Honeycutt 1995) and $13.^{m}84$ for R filter (Pelle 2005).

In order to find the periods embedded in this system, a periodogram $S(f)$ is calculated. The test function $S(f)$ is the square of the correlation coefficient between the observations and the values calculated using sine fit with a trial frequency (see Andronov 1994, 2003 for details). Fig. 2 shows the orbital light curves (left) and periodogram (right) for observation days showing QPO in our data.

3. QUASI PERIODIC OSCILLATION

For QPOs observed in polar-type MCVs, observation and numerical calculation results have been reported (Bonnet-Bidaud et al. 2015; Busschaert et al. 2015), however, there is no report on qualitative and quantitative model calculation results for IP-type MCVs, yet. Thus, it is of significance to sort out the characteristics observed in these stars.

Mateo et al. (1991) have discovered the rotation period

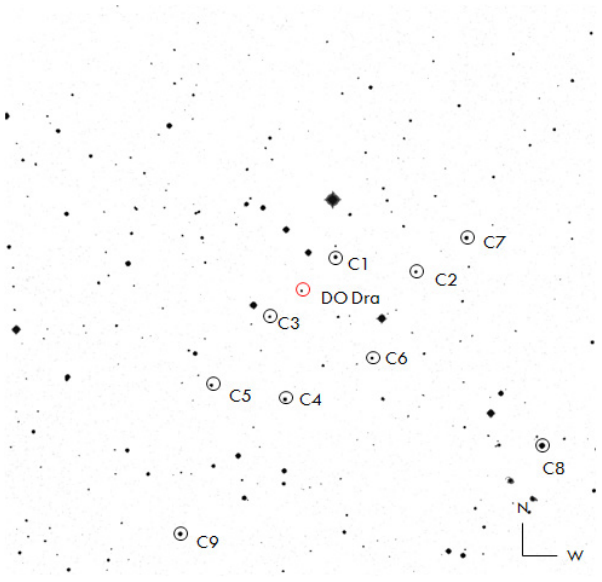

Fig. 1. The finding map of DO Dra with the size of 22'.2 × 22'.2.

of 14.2 min (852 sec) which is longer than the other rotation periods from the one-day observation data with B filter. Also, Andronov et al. (2008) have discovered the period of 30.4 min (1,824 sec) which is approximately twice the period determined by Mateo et al. In this study, in order to analyze the periods of various QPOs, we have selected days showing significant variations in light intensity on the light curves. For these selected days, we have generated light curves and periodograms and those are presented in Fig. 2. In the light curves on the left of Fig. 2, we can see magnitude oscillations with periods different from the rotation period or the revolution period. On HJD 2454178, the significant variations of magnitude were observed with the maximum amplitude of 0.4. Subsequently, QPOs have been observed for HJD 2454191 to HJD 2454194. On HJD 2454197, QPOs were not observed at first but started to appear from the middle of data and on HJD 2456000, we can see magnitude variations became relatively small. In this figure, the eclipse timing of QPOs observed on HJD 2454163, HJD 2454178, and HJD 2454191 are indicated with the short vertical bar. The first vertical solid line on the right plot of Fig.2 indicates the approximate frequency of $f \approx 17.5$ cycles/day; the second line and the third line represent $f \approx 28$ cycles/day, $f \approx 44$ cycles/day, respectively; the fourth line indicates $f \approx 47.5$ cycles/day discovered by Andronov et al. (2008). Around the solid lines drawn, several similar periods were discovered. For the consecutive days of HJD 2453191 through HJD 2453194, the light curves show similar periodic behavior.

Table 1. Information on DO Dra and comparison stars

Star	RA	Dec(+)	V	B-V	V-R
DO Dra*	$11^h\,43^m\,38^s$	71° 41' 20"	$14.^m755$	$0.^m106$	$0.^m666$
C1	$11^h\,43^h\,23^h$	71° 42' 43"	$14.^m272$	$0.^m802$	$0.^m467$
C2	$11^h\,42^m\,44^s$	71° 42' 21"	$15.^m306$	$0.^m629$	$0.^m322$
C3	$11^h\,43^m\,52^s$	71° 40' 14"	$15.^m761$	$0.^m685$	$0.^m411$
C4	$11^h\,43^m\,42^s$	71° 37' 05"	$14.^m325$	$1.^m080$	$0.^m641$
C5	$11^h\,44^m\,17^s$	71° 37' 24"	$15.^m175$	$1.^m011$	$0.^m616$
C6	$11^h\,43^m\,02^s$	71° 38' 53"	$15.^m181$	$0.^m667$	$0.^m393$
C7	$11^h\,42^m\,21^s$	71° 43' 48"	$13.^m835$	$0.^m582$	$0.^m337$
C8	$11^h\,41^m\,38^s$	71° 35' 55"	$12.^m183$	$0.^m846$	$0.^m481$
C9	$11^h\,44^m\,27^s$	71° 31' 33"	$13.^m390$	$0.^m609$	$0.^m350$
C10	$11^h\,45^m\,23^s$	71° 26' 42"			
C11*	$11^h\,48^m\,36^s$	71° 07' 50"	$14.^m25$	$1.^m28$	$-0.^m45$
C12*	$11^h\,40^m\,30^s$	71° 11' 02"	$13.^m76$	$0.^m73$	$-0.^m4$
C13*	$11^h\,40^m\,48^s$	71° 11' 04"			
C14	$11^h\,40^m\,45^s$	71° 10' 30"			
C15	$11^h\,40^m\,44^s$	71° 14' 08"			
C16	$11^h\,40^m\,50^s$	71° 15' 22"			
C17	$11^h\,40^m\,27^s$	71° 14' 16"			
C18	$11^h\,40^m\,09^s$	71° 14' 18"			
C19	$11^h\,39^m\,37^s$	71° 15' 46"			
C20	$11^h\,41^m\,22^s$	71° 12' 20"			

* Represents CVs. The location of stars are obtained from the Wenger et al. (2014). The magnitude information is obtained from Kafka (2016).

Table 2 shows the measured QPO periods from the periodogram analysis of light curves as suggested by Andronov (2003) for the individual days where QPOs were observed. According to the period information summarized in this table, the period of QPOs ranges $P_{QPOs} = 30^m \sim 80^m$, we can conclude that QPOs do not occur always and the periods of QPOs are changing.

The individual days where QPOs are observed clearly can be found by calculating the periodogram $S(f)$. In the left plot of Fig. 2, the calculated times of maximum are indicated with the short vertical bar for 3 days of HJD 2454163, HJD 2454178, and HJD 2454191 which show clear periodic behavior compared to others. Using the times of maximum, as the epoch time, T_0, and the periods of the QPO period, P_{QPOs} for the individual QPOs are estimated as shown below.

$$T_0 = \text{HJD } 2454163.9273(15)$$
$$P_{QPOs} = 0.^d0211168(15) \text{ for HJD } 2454163$$
$$T_0 = \text{HJD } 2454178.8776(15)$$
$$P_{QPOs} = 0.^d0357537(1) \text{ for HJD } 2454178$$
$$T_0 = \text{HJD } 2454191.8327(9)$$
$$P_{QPOs} = 0.^d0251576(7) \text{ for HJD } 2453191$$

Using these light elements of QPOs determined separately, folded light curves are presented in Fig. 3.

4. DISCUSSION

Although QPOs had been identified clearly during the ten year long observation of DO Dra, it was difficult to get any general statistical conclusions on the periodicity. From the fact

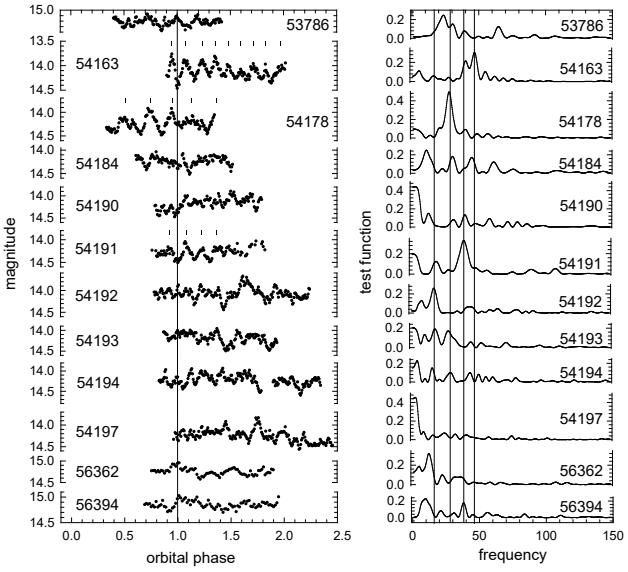

Fig. 2. The orbital light curves (left) and periodogram (right) for observation days showing QPO; The number of the figure indicates the observed day in in HJD-2400000.

Table 2. Periods of QPOs estimated from the periodogram analysis

HJD 24+	f	σ_f	r (mag)	σ_r	P (day)	P (min)
53786	23.54	0.43	0.043	0.0046	0.0424720	61.16
54163	47.35	0.34	0.101	0.0117	0.0211172	30.41
54178	27.97	0.28	0.129	0.0077	0.0357542	51.49
54184	30.53	0.63	0.055	0.0076	0.0327540	47.17
54190	40.04	0.60	0.065	0.0103	0.0249774	35.97
54191	39.75	0.44	0.087	0.0116	0.0251581	36.28
54192	17.60	0.26	0.092	0.0108	0.0568048	81.80
54193	17.94	0.57	0.078	0.0092	0.0557268	80.25
54194	43.90	0.53	0.057	0.0084	0.0227803	32.80
54197	24.55	0.98	0.053	0.0097	0.0407298	58.65
56362	36.41	2.78	0.031	0.0087	0.0274663	39.55
56394	38.09	0.60	0.041	0.0070	0.0262517	37.80

The numer in the first coulum is the observed day in HJD-2400000. f indicates the frequency with its standard deviation σ_f and r is the semi-amplitude with its standard deviation σ_r. The estimated period P is shown in two units(day and minunte).

that the interval of the observation showing QPO, it is obvious that the period ranges between 13 day and 15 day. We have checked whether there is a distinct QPO period in this range. A least square analysis has been carried out for the periodicity as shown in Table 2, starting from a period of 13 day up to 15 day with the increment of 0.01 day. It is interesting that the QPO behavior seems to repeat itself in 13.52 day, although this result should be confirmed in the future analysis to be more accurate. In this process, HJD 2456362 and HJD 2456394 were excluded because of the accumulated error propagation. The QPO periods presented in Table 2 are superposed with sine curve with the period of 13.52 day and presented in Fig. 4. Andronov et al. (2008) pointed out that various QPOs and transient periodic oscillations (TPOs) exist in the observational data, but they could not found some periodicity of these QPOs. At this time, the observational data are not sufficient to confirm this periodicity. Therefore, further monitoring observation is necessary to clearly identify this period variation.

There have been several attempts to explain the QPO models identified in the optical and X-ray light curves observed in polar-type stars with strong magnetic fields (Bonnet-Bidaud et al. 2015; Busschaert et al. 2015), however, calculation models of IP-type stars with accretion disk are so complicated that the explanations were not ever made yet. But a lot of QPOs have been observed in these stars, and it is believed that the periods depend on the various elements such as accretion disk, the change in accretion rate of mass which passes the magnetic sphere of white dwarfs, etc., and that the amplitude of QPOs will display variations.

In order to see this dependence, the semi-amplitude and the QPO period in Table 2 are plotted for the days showing the obvious QPO. It can be concluded from Fig. 5 that the semi-amplitude increases as the QPO period becomes longer, even though this is hard to be confirmed due to lack of data. However, this trend can be used as initial data for magnetic field change or accretion rate change in the future model calculation to enable observational verification of theory. In order to achieve this purpose, continuous monitoring and analysis related to the variation of QPO periods are essential.

Assuming that blobs located between white dwarfs and accretion disks constitute one of the various causes of QPO, the location of blobs can be estimated from the Kepler's law. Blobs are believed to change periodically between the maximum distance of $R_{blobs} = R_{wd} \cdot 9.27^{2/3} = 4.41 R_{wd}$ and the minimum distance of $2.28 R_{wd}$ (Andronov et al. 2008) or of $1.39 R_{wd}$ (Mateo et al. 1991). However, it is worth mentioning that QPOs do not occur always and occasionally, they show transient behavior of which mechanism is not clear to be explained yet.

Based on the results of light elements determined for QPOs observed on HJD 2454163, HJD 2454178, and HJD 2454191, it can be concluded that QPOs occur with the period of 13.52 day. However, it is not possible to explain this behavior of QPOs with unsteady amplitudes and periods at this time. Further monitoring observations will enable us to analyze more accurately, and understand the physical condition of radiative region of the magnetic cataclysmic variables.

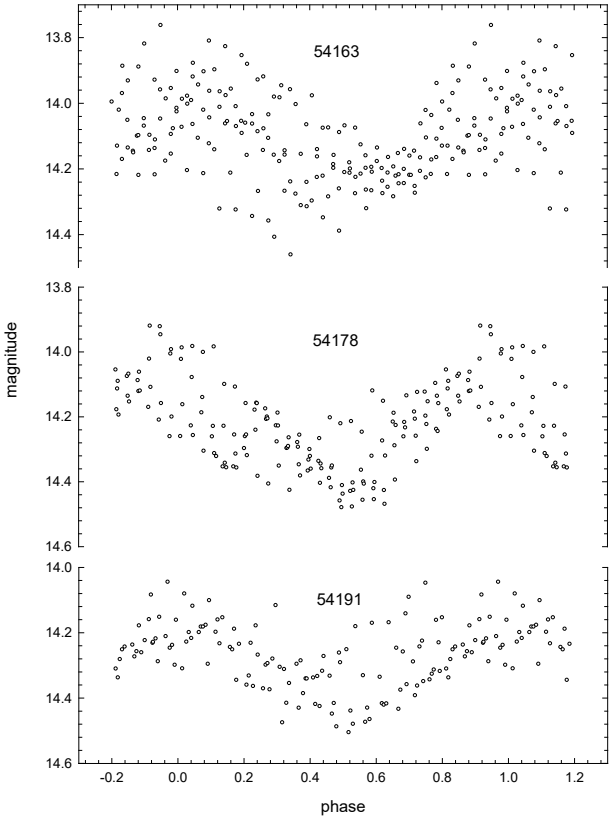

Fig. 3. The light curve with the QPO period for individual day. The number of the figure indicates the observed day in HJD-2400000.

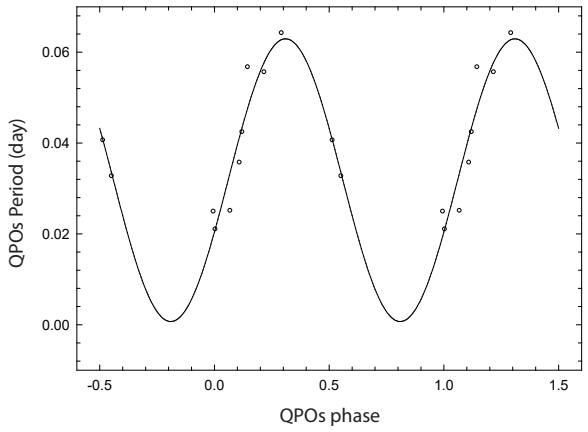

Fig. 4. The variation of the QPO period in QPO phase. The data are fitted with the sine curve of the period of 13.52 day.

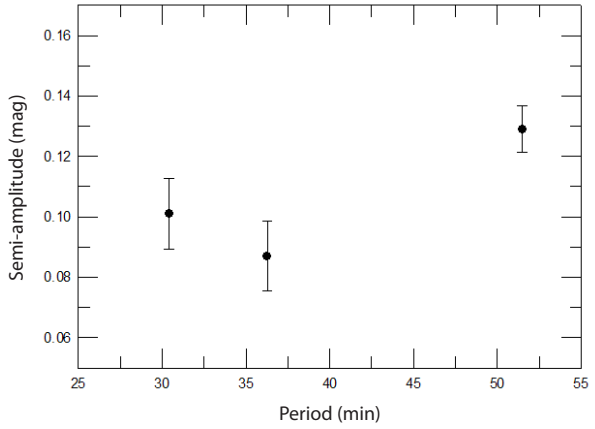

Fig. 5. The relation of the semi-amplitude and the period for some QPOs which show obvious periodic behavior. The data points and error bar are from the Table 2.

ACKNOWLEDGMENTS

This work was supported by the research grant of Chungbuk National University in 2014. The data acquisition and analysis was partially supported by Basic Science Research Program through the National Research Foundation of Korea (NRF) funded by the Ministry of Education, Science and Technology (2011-0014954). It is also a part of the "Inter-Longitude Astronomy" campaign (Andronov et al. 2010).

REFERENCES

Andronov IL, (Multi-) frequency variations of stars. some methods and results, Odessa Astron. Publ. 7, 49-54 (1994).

Andronov IL, Multiperiodic versus noise variations: mathematical methods, Astron. Soc. Pac. Conf. Ser. 292, 391-400 (2003).

Andronov IL, Baklanov AV, Algorithm of the artificial comparison star for the CCD photometry, Astron. Sch. Rep. 5, 264-272 (2004).

Andronov IL, Arai K, Chinarova LL, Dorokhov NI, Dorokhova TN, et al., A search for periodic and quasi-periodic photometric behavior in the cataclysmic variable TT Arietis, Astron. J. 117, 574-586 (1999). https://dx.doi.org/10.1086/300665

Andronov IL, Chinarova LL, Han W, Kim Y, Yoon JN, Multiple timescales in cataclysmic binaries, Astron. Astrophys. 486, 855-865 (2008). https://dx.doi.org/10.1051/0004-6361:20079056

Andronov IL, Antoniuk KA, Baklanov AV, Breus VV, Burwitz V, et al., "Inter-longitude astronomy" (ILA) project: current highlights and perspectives. I. magnetic vs. non-magnetic interacting binary stars, Odessa Astron. Publ. 23, 8-10 (2010). https://dx.doi.org/10.18524/1810-4215.2010.23.84023

Andronov IL, Kim Y, Yoon JN, Breus VV, Smecker-Hane TA, et al., Two-color CCD photometry of the intermediate polar 1RXS J180340.0+401214, J. Korean Astron. Soc. 44, 89-96 (2011). https://dx.doi.org/10.5303/JKAS.2011.44.3.89

Andronov IL, Kim Y, Kim YH, Yoon JN, Chinarova LL, et al., Phenomenological modeling of newly discovered eclipsing binary 2MASS J18024395+4003309=VSX J180243.9+400331, J. Astron. Space Sci. 32, 127-136 (2015). https://dx.doi.org/10.5140/JASS.2015.32.2.127

Bonnet-Bidaud JM, Mouchet M, Busschaert C, Falize E, Michaut C, Quasi-periodic oscillations in accreting magnetic white dwarfs I. observational constraints in X-ray and optical, Astron. Astrophys. 579, A24 (2015). https://dx.doi.org/10.1051/0004-6361/201425482

Busschaert C, Falize É, Michaut C, Bonnet-Bidaud JM, Mouchet M, Quasi-periodic oscillations in accreting magnetic white dwarfs II. The asset of numerical modelling for interpreting observations, Astron. Astrophys. 579, A25 (2015). https://dx.doi.org/10.1051/0004-6361/201425483

Haswell CA, Patterson J, Thorstensen JR, Hellier C, Skillman DR, Pulsations and accretion geometry in YY Draconis: a study based on *Hubble Space Telescope* observations, Astrophys. J. 476, 847-864 (1997). https://dx.doi.org/10.1086/303630

Henden AA, Honeycutt RK, Secondary photometric standards for northern nova-like cataclysmic variables, Publ. Astron. Soc. Pac. 107, 324-346 (1995).

Kafka S, Observation from the AAVSO International Database [Internet], cited 2016, available from: https://www.aavso.org

Kim Y, Andronov IL, Jeon YB, CCD photometry using multiple comparison stars, J. Astron. Space Sci. 21, 191-200 (2004). https://dx.doi.org/10.5140/JASS.2004.21.3.191

Kim Y, Andronov IL, Park SS, Chinarova LL, Baklanov AV, et al.,

Two-color VR CCD photometry of the intermediate polar 1RXS J062518.2+733433, J. Astron. Space Sci. 22, 197-210 (2005a) https://dx.doi.org/10.5140/JASS.2005.22.3.197

Kim Y, Andronov IL, Park SS, Jeon YB, Orbital and spin variability of the intermediate polar BG CMi, Astron. Astrophys. 441, 663-674 (2005b). https://dx.doi.org/10.1051/0004-6361:20052995

Kim Y, Andronov IL, Cha SM, Chinarova LL, Yoon JN, Nova-like cataclysmic variable TT Arietis QPO behavior coming back from positive superhumps, Astron. Astrohpys. 496, 765-775 (2009).

Massey P, Davis LE, A user's guide to stellar CCD photometry with IRAF (NOAO Laboratory, Tucson, 1992).

Mateo M, Szkody P, Garnavich P, Near-infrared time-resolved spectroscopy of the cataclysmic variable YY Draconis, Astrophys. J. 370, 370-383 (1991).

Norton AJ, Beardmore AP, Allan A, Hellier C, YY Draconis and V709 Cassiopeiae: two intermediate polars with weak magnetic fields, Astron. Astrophys. 347, 203-211 (1999).

Patterson J, Schwartz DA, Bradt H, Remillard RA, McHardy IM, et al., Identification of the bright X-ray source 3A1148+719 with the cataclysmic variable YY Draconis, Bull. Am. Astron. Soc. 14, 618 (1982).

Patterson J, Schwartz DA, Pye JP, Blair WP, Williams GA, et al., Rapid oscillations in cataclysmic variables. VIII – YY Draconis (3A 1148+719), Astrophys. J. 392, 233-242 (1992).

Pelle JC, Field 11436p7142 for SN 2005cz [Internet], cited 2005, available from: http://www.astrosurf.com/snweb2/2005/05cz/05czPhot.htm

Remillard RA, Muno MP, McClintock JE, Orosz JA, New views on microquasars: proceedings of the Fourth Microquasars Workshop, Institut d'Études Scientifiques de Cargèse, Corse, France, 27 May – 1 June 2002.

Samus NN, Kazarobets EV, Durlevich OV, Kireeva NN, Patukhova EN, General catalogue of variable stars: version CGVS 5.1, Astron. Rep. 61, 80-88 (2017). https://dx.doi.org/10.1134/S1063772917010085

Šimon V, Outburst activity of the intermediate polar DO Draconis (3A 1148+719), Astron. Astrophys. 360, 627-632 (2000).

Smak J, TT Ari and quasi-periodic oscillations, Acta Astron. 64, 167-175 (2014).

Tremko J, Andronov IL, Chinarova LL, Kumsiashvili MI, Luthardt R, et al., Periodic and aperiodic variations in TT Arietis- results from an international campaign, Astron. Astrophys. 312, 121-134 (1996).

Wenger M, Ochsenbein F, Egret D, Dubois P, Bonnarel F, et al., The SIMBAD astronomical database- the CDS reference database for astronomical objects, Astron. Astrophys. Suppl. Ser. 143, 9-22 (2000). https://dx.doi.org/10.1051/aas:2000332

Wenzel W, The X-ray source 3A1148+719 is another dwarf nova with very long cycle length, Inf. Bull. Var. Stars 2262, 1-2 (1983).

Yun A, Kim Y, Choi C, Long-term variation of the spin period of a magnetic cataclysmic variable, MU Camelopardalis, J. Astron. Space Sci. 28, 9-12 (2011). https://dx.doi.org/10.5140/JASS.2011.28.1.009

APPENDIX I

Journal of observations of DO Dra at LOAO: Beginning t_{begin} and ending t_{end} times in HJD-2400000, of observations; Number of observations n; Magnitude range for individual data points m_{max}, m_{min}; Nightly mean <m> and its accuracy estimate, r.m.s. deviation of the single observation from the mean $\sigma(m)$, and the used filter.

t_{begin} - t_{end}	n	range	<m>	$\sigma(m)$	filter
56309.991~.062	11	15.680 ~ 16.006	15.850 ± 0.030	0.100	B
56310.796~.058	43	15.712 ~ 15.999	15.866 ± 0.013	0.082	B
56311.976~.061	13	15.686 ~ 15.930	15.801 ± 0.019	0.069	B
56314.868~.063	30	15.504 ~ 15.805	15.622 ± 0.016	0.089	B
56315.745~.053	50	15.442 ~ 15.891	15.641 ± 0.013	0.090	B
56316.707~.803	14	15.455 ~ 15.764	15.612 ± 0.024	0.089	B
56671.803~.059	42	15.942 ~ 16.361	16.124 ± 0.017	0.109	B
56673.804~.048	49	16.216 ~ 16.661	16.416 ± 0.017	0.120	B
54478.027~.066	23	14.020 ~ 14.658	14.291 ± 0.031	0.149	V
54478.772~.066	139	13.984 ~ 14.676	14.330 ± 0.014	0.169	V
54479.880~.068	53	13.948 ~ 14.632	14.372 ± 0.020	0.147	V
54480.736~.768	20	14.129 ~ 14.549	14.355 ± 0.027	0.122	V
54481.967~.010	14	14.151 ~ 14.457	14.304 ± 0.023	0.086	V
54482.928~.957	16	14.088 ~ 14.663	14.362 ± 0.044	0.177	V
54484.057~.067	7	14.115 ~ 14.371	14.210 ± 0.029	0.078	V
54485.044~.066	14	13.905 ~ 14.708	14.327 ± 0.069	0.258	V
54486.041~.067	16	14.238 ~ 14.564	14.437 ± 0.022	0.088	V
54487.051~.069	10	14.116 ~ 14.659	14.351 ± 0.064	0.202	V
54904.882~.994	44	15.199 ~ 15.702	15.428 ± 0.021	0.139	V
54905.872~.039	59	15.136 ~ 15.580	15.380 ± 0.012	0.092	V
54906.870~.036	76	15.242 ~ 15.780	15.506 ± 0.014	0.124	V
54907.863~.036	81	15.196 ~ 15.657	15.454 ± 0.011	0.101	V
54908.888~.036	54	15.209 ~ 15.594	15.400 ± 0.012	0.090	V
54909.861~.034	81	15.186 ~ 15.651	15.405 ± 0.012	0.107	V
55566.827~.064	30	15.434 ~ 15.862	15.667 ± 0.016	0.088	V
55569.990~.064	11	15.763 ~ 16.077	15.954 ± 0.031	0.103	V
55931.872~.057	25	15.437 ~ 15.641	15.541 ± 0.011	0.055	V
55932.894~.975	12	15.593 ~ 15.752	15.679 ± 0.016	0.054	V
55933.862~.054	25	15.496 ~ 15.680	15.593 ± 0.010	0.052	V
55952.811~.061	31	15.413 ~ 15.584	15.504 ± 0.008	0.042	V
55953.812~.043	31	15.314 ~ 15.585	15.418 ± 0.011	0.062	V
55957.817~.965	12	15.420 ~ 15.636	15.511 ± 0.019	0.067	V
55997.802~.824	4	15.935 ~ 15.992	15.957 ± 0.013	0.026	V
55998.767~.883	14	15.660 ~ 15.851	15.752 ± 0.014	0.054	V
55999.772~.862	13	15.658 ~ 15.774	15.712 ± 0.012	0.042	V
56000.776~.931	20	15.415 ~ 15.701	15.575 ± 0.017	0.076	V
56001.761~.861	13	15.424 ~ 15.694	15.512 ± 0.020	0.073	V
56002.728~.906	24	15.311 ~ 15.582	15.419 ± 0.013	0.065	V
56309.994~.064	10	15.467 ~ 15.732	15.627 ± 0.027	0.087	V
56310.799~.060	40	15.510 ~ 15.763	15.636 ± 0.010	0.064	V
56311.978~.063	13	15.417 ~ 15.759	15.595 ± 0.022	0.080	V
56313.969~.059	14	15.355 ~ 15.746	15.547 ± 0.026	0.096	V
56314.871~.065	32	15.278 ~ 15.599	15.401 ± 0.016	0.092	V
56315.747~.056	49	15.216 ~ 15.656	15.410 ± 0.013	0.092	V
56316.710~.798	12	15.243 ~ 15.521	15.372 ± 0.024	0.085	V
56671.805~.062	43	15.763 ~ 16.068	15.922 ± 0.010	0.067	V
56673.806~.045	41	15.918 ~ 16.340	16.123 ± 0.018	0.114	V
53672.996~.031	38	14.207 ~ 14.550	14.362 ± 0.017	0.104	R
53693.047~.047	1	15.430 ~ 15.430	15.430 ± 0.000	0.000	R
53694.029~.044	2	15.411 ~ 15.544	15.478 ± 0.067	0.094	R
53695.026~.026	1	15.663 ~ 15.663	15.663 ± 0.000	0.000	R
53752.898~.071	91	14.969 ~ 15.223	15.124 ± 0.006	0.056	R
53753.876~.055	78	15.061 ~ 15.352	15.220 ± 0.009	0.077	R
53774.865~.061	27	12.405 ~ 12.771	12.607 ± 0.018	0.091	R
53780.841~.841	1	15.159 ~ 15.159	15.159 ± 0.000	0.000	R
53782.029~.065	30	15.106 ~ 15.376	15.236 ± 0.011	0.059	R
53786.885~.053	138	14.846 ~ 15.376	15.211 ± 0.004	0.071	R
54161.889~.999	60	14.117 ~ 14.515	14.287 ± 0.011	0.087	R
54162.879~.038	153	13.802 ~ 14.600	14.217 ± 0.012	0.151	R
54163.854~.039	176	13.762 ~ 14.460	14.116 ± 0.010	0.130	R
54178.810~.978	146	13.919 ~ 14.478	14.241 ± 0.011	0.128	R
54184.809~.959	119	14.037 ~ 14.516	14.239 ± 0.009	0.093	R
54190.792~.958	132	13.896 ~ 14.474	14.169 ± 0.011	0.125	R
54191.780~.955	118	14.030 ~ 14.504	14.276 ± 0.010	0.107	R
54192.776~.017	210	13.673 ~ 14.441	14.071 ± 0.009	0.127	R
54193.782~.959	154	13.959 ~ 14.492	14.191 ± 0.010	0.125	R
54194.767~.018	204	13.932 ~ 14.594	14.226 ± 0.009	0.126	R
54195.737~.010	113	13.957 ~ 14.432	14.245 ± 0.010	0.106	R
54196.896~.985	65	13.949 ~ 14.310	14.123 ± 0.010	0.080	R
54197.767~.014	195	13.829 ~ 14.560	14.252 ± 0.010	0.140	R
54198.749~.813	50	13.865 ~ 14.299	14.119 ± 0.015	0.103	R
54201.757~.809	43	14.073 ~ 14.335	14.202 ± 0.009	0.060	R
54477.018~.064	28	14.098 ~ 14.351	14.227 ± 0.012	0.063	R
54478.027~.066	23	13.603 ~ 14.123	13.840 ± 0.025	0.120	R
54478.773~.066	145	13.578 ~ 14.184	13.861 ± 0.013	0.151	R
54479.881~.069	53	13.472 ~ 14.093	13.886 ± 0.018	0.134	R
54480.736~.769	20	13.704 ~ 14.048	13.886 ± 0.021	0.096	R
54481.977~.011	16	13.720 ~ 14.001	13.881 ± 0.022	0.090	R
54482.928~.959	15	13.699 ~ 14.124	13.896 ± 0.035	0.137	R
54484.058~.068	7	13.639 ~ 13.838	13.745 ± 0.029	0.077	R
54485.044~.067	14	13.625 ~ 14.169	13.852 ± 0.054	0.204	R
54486.042~.068	16	13.790 ~ 14.075	13.956 ± 0.022	0.090	R
54487.051~.070	11	13.680 ~ 14.124	13.877 ± 0.046	0.153	R
54901.883~.043	120	14.699 ~ 15.120	14.902 ± 0.008	0.089	R
54902.885~.908	14	14.865 ~ 15.088	14.949 ± 0.017	0.063	R
54904.881~.995	43	14.693 ~ 15.148	14.907 ± 0.020	0.131	R
54905.870~.040	63	14.671 ~ 15.032	14.842 ± 0.011	0.085	R
54906.871~.037	75	14.732 ~ 15.183	14.956 ± 0.014	0.120	R
54907.864~.035	80	14.698 ~ 15.077	14.902 ± 0.010	0.087	R
54908.887~.037	55	14.698 ~ 15.027	14.859 ± 0.010	0.076	R
54909.862~.035	81	14.613 ~ 15.064	14.856 ± 0.010	0.092	R
55566.831~.068	30	14.833 ~ 15.211	15.070 ± 0.015	0.080	R
55569.994~.053	9	15.228 ~ 15.661	15.397 ± 0.042	0.126	R
55931.875~.061	23	14.907 ~ 15.040	14.981 ± 0.008	0.039	R
55932.897~.978	12	15.043 ~ 15.173	15.096 ± 0.011	0.037	R
55933.866~.057	25	14.919 ~ 15.155	15.064 ± 0.010	0.050	R
55952.815~.065	32	14.874 ~ 15.019	14.938 ± 0.006	0.036	R
55953.816~.046	30	14.765 ~ 14.987	14.885 ± 0.009	0.051	R
55957.813~.968	14	14.877 ~ 15.083	14.952 ± 0.017	0.063	R
55997.806~.820	3	15.324 ~ 15.346	15.335 ± 0.006	0.011	R
55998.770~.879	13	15.050 ~ 15.266	15.185 ± 0.014	0.050	R
55999.776~.859	12	15.060 ~ 15.161	15.119 ± 0.010	0.036	R
56000.780~.927	19	14.871 ~ 15.106	14.997 ± 0.016	0.069	R
56001.765~.858	11	14.846 ~ 15.068	14.952 ± 0.020	0.067	R
56002.731~.902	24	14.793 ~ 15.013	14.867 ± 0.011	0.055	R
56309.006~.053	14	14.951 ~ 15.103	15.002 ± 0.013	0.049	R
56309.995~.066	11	14.903 ~ 15.178	15.052 ± 0.029	0.097	R
56310.800~.062	42	14.961 ~ 15.219	15.068 ± 0.010	0.067	R
56311.980~.065	14	14.986 ~ 15.132	15.041 ± 0.013	0.047	R
56313.971~.055	12	14.871 ~ 15.135	14.977 ± 0.021	0.074	R
56314.872~.067	30	14.748 ~ 15.080	14.895 ± 0.014	0.078	R
56315.749~.063	49	14.734 ~ 15.066	14.899 ± 0.012	0.081	R
56316.711~.800	11	14.769 ~ 15.013	14.870 ± 0.023	0.075	R
56671.807~.063	43	15.133 ~ 15.409	15.297 ± 0.010	0.067	R
56673.808~.046	41	15.330 ~ 15.682	15.501 ± 0.014	0.092	R

APPENDIX II

Journal of observations of DO Dra at CBNUO: Beginning t_{begin} and ending t_{end} times in HJD-2400000, of observations; Number of observations n; Magnitude range for individual data points m_{max}, m_{min}; Nightly mean <m> and its accuracy estimate, r.m.s. deviation of the single observation from the mean $\sigma(m)$, and the used filter.

t_{begin} - t_{end}	n	range	<m>	$\sigma(m)$	filter
55693.038~.160	32	14.646 ~ 14.873	14.775 ± 0.012	0.069	R
55697.995~.207	50	14.609 ~ 14.814	14.708 ± 0.006	0.043	R
55699.023~.141	32	14.487 ~ 14.749	14.590 ± 0.011	0.065	R
56272.308~.399	13	14.946 ~ 15.102	15.060 ± 0.011	0.039	R
56346.281~.388	26	14.420 ~ 14.807	14.623 ± 0.016	0.079	R
56353.284~.365	20	14.836 ~ 15.028	14.917 ± 0.012	0.052	R
56355.143~.298	43	14.817 ~ 15.104	14.957 ± 0.010	0.067	R
56357.016~.361	138	14.797 ~ 15.125	14.968 ± 0.005	0.063	R
56360.143~.274	53	14.592 ~ 15.005	14.794 ± 0.011	0.079	R
56362.147~.336	76	14.578 ~ 14.958	14.753 ± 0.009	0.079	R
56363.148~.302	62	14.599 ~ 14.988	14.763 ± 0.013	0.102	R
56366.137~.250	46	14.594 ~ 15.054	14.869 ± 0.017	0.113	R
56367.143~.173	13	14.698 ~ 14.964	14.820 ± 0.026	0.093	R
56372.985~.086	41	14.552 ~ 14.909	14.775 ± 0.011	0.073	R
56394.053~.261	83	14.702 ~ 15.026	14.853 ± 0.008	0.070	R
56395.019~.206	75	14.685 ~ 14.996	14.837 ± 0.007	0.062	R
56398.132~.200	28	14.529 ~ 14.781	14.679 ± 0.011	0.058	R
56401.031~.153	49	14.821 ~ 15.175	15.010 ± 0.008	0.057	R
56406.973~.059	35	14.797 ~ 15.244	15.068 ± 0.020	0.117	R
56408.967~.134	67	14.733 ~ 15.136	14.950 ± 0.009	0.077	R
56411.963~.137	68	14.561 ~ 15.063	14.855 ± 0.013	0.106	R
56412.961~.130	68	14.733 ~ 15.033	14.915 ± 0.007	0.061	R
56428.999~.103	42	14.900 ~ 15.186	15.027 ± 0.011	0.068	R
56432.975~.075	41	15.114 ~ 15.398	15.238 ± 0.010	0.065	R
56433.971~.079	42	14.958 ~ 15.342	15.154 ± 0.014	0.092	R
56442.982~.059	31	14.792 ~ 15.168	14.941 ± 0.015	0.085	R
56447.980~.012	14	14.994 ~ 15.308	15.139 ± 0.026	0.097	R
56650.289~.407	33	14.707 ~ 14.922	14.810 ± 0.011	0.062	R
56651.271~.408	72	14.585 ~ 14.968	14.764 ± 0.008	0.071	R
56654.276~.409	91	15.351 ~ 16.121	15.711 ± 0.019	0.183	R
56658.217~.406	53	14.869 ~ 15.223	15.058 ± 0.012	0.086	R
56659.230~.412	71	14.972 ~ 15.344	15.116 ± 0.009	0.074	R
56660.330~.399	26	14.617 ~ 15.288	15.038 ± 0.031	0.160	R
56664.327~.412	30	14.984 ~ 15.386	15.134 ± 0.015	0.082	R
56667.201~.344	47	14.893 ~ 15.202	15.032 ± 0.010	0.071	R
56686.256~.405	58	15.800 ~ 16.207	16.011 ± 0.012	0.092	R
56709.152~.180	10	15.373 ~ 15.594	15.452 ± 0.019	0.061	R
56710.149~.391	80	15.188 ~ 16.019	15.458 ± 0.017	0.155	R